

Axion as a cold dark matter candidate: low-mass case

Chan-Gyung Park¹, Jai-chan Hwang^{2,3}, and Hyerim Noh¹

¹*Korea Astronomy and Space Science Institute, Daejeon 305-348, Republic of Korea*

²*Department of Astronomy and Atmospheric Sciences,*

Kyungpook National University, Daegu 702-701, Republic of Korea

³*Korea Institute for Advanced Study, Seoul 130-722, Republic of Korea*

(Dated: July 16, 2012)

Axion as a coherently oscillating scalar field is known to behave as a cold dark matter in all cosmologically relevant scales. For conventional axion mass with 10^{-5} eV, the axion reveals a characteristic damping behavior in the evolution of density perturbations on scales smaller than the solar system size. The damping scale is inversely proportional to the square-root of the axion mass. We show that the axion mass smaller than 10^{-24} eV induces a significant damping in the baryonic density power spectrum in cosmologically relevant scales, thus deviating from the cold dark matter in the scale smaller than the axion Jeans scale. With such a small mass, however, our basic assumption about the coherently oscillating scalar field is broken in the early universe. This problem is shared by other dark matter models based on the Bose-Einstein condensate and the ultra-light scalar field. We introduce a simple model to avoid this problem by introducing evolving axion mass in the early universe, and present observational effects of present-day low-mass axion on the baryon density power spectrum, the cosmic microwave background radiation (CMB) temperature power spectrum, and the growth rate of baryon density perturbation. In our low-mass axion model we have a characteristic small-scale cutoff in the baryon density power spectrum below the axion Jeans scale. The small-scale deviations from the cold dark matter model in both matter and CMB power spectra clearly differ from the ones expected in the cold dark matter model mixed with the massive neutrinos as a hot dark matter component.

PACS numbers: 98.80.-k, 95.35.+d

I. INTRODUCTION

Observations of type Ia supernovae, cosmic microwave background (CMB) radiation anisotropy, and large-scale structure of galaxies have revealed that our present universe is dominated by two dark components [1]. Based on the Friedmann world model, the energy content of the present universe is occupied by 73% of dark energy and 23% of dark matter, whose nature is the fundamental mystery of the present day theoretical physics and cosmology (see Ref. [2] for recent cosmological interpretation of astronomical observations).

The dark matter is often modeled as pressureless, non-relativistic particles, which is known as cold dark matter (CDM). Although the CDM model has been greatly successful in explaining many cosmological observations, there remain certain conflicts at the galactic scales. First, the CDM-based simulations of galactic halos show density profiles with a central cusp at kpc scale, while observations indicate constant density cores [3]. Secondly, the CDM model predicts overpopulation of low mass halos within a galaxy or a galaxy group, which is an order of magnitude larger than the present observations [4].

These CDM problems at galactic scales may be overcome by introducing a suppression of small-scale power in the density perturbation. There have been efforts to explain the CDM conflicts using the dark matter models with the Bose-Einstein condensate (BEC) and the ultra-light scalar field.

In the BEC dark matter model the bosonic particles occupy the lowest quantum state of the external potential

and can be described as a coherent matter wave of macroscopic size due to Bose enhancement [5–10]. Along this line there is fuzzy cold dark matter model proposed by Hu et al. [11] which is a case of free particles ignoring the self-interaction terms in the BEC based on the generalized dark matter approach [12]. In this model the coherent wave of ultra-light dark matter with $m \sim 10^{-22}$ eV can suppress the kpc-scale cusp in the dark matter halos and reduce the abundance of low mass halos. Recent investigations on the growth of perturbation in the universe with BEC dark matter can be found in Refs. [9, 10]. The BEC dark matter has a close connection to the axion dark matter model. Recently, Sikivie and Yang [13] showed that the cold dark matter axions form a BEC through their self-interactions and gravitational interactions (see also Ref. [14]).

Another possibility is the ultra-light scalar field dark matter model [15–24] (see Ref. [25] for a review). Based on a specific scalar field potential with appropriate initial conditions the evolution of scalar field mimics the property of the CDM fluid. For example, authors of Refs. [17, 18] proposed cosh-like potential $V = V_0(\cosh \lambda\phi - 1)$ as a good candidate of dark matter (see also Ref. [20]). Authors of Refs. [21, 22] investigated the structure formation in the scalar-field dark matter model with $V = \frac{1}{2}m^2\phi^2 + \frac{1}{4}\lambda\phi^4$ by using the fluid and the field approaches. Authors of Refs. [23, 24] studied the effect of ultra-light scalar field with $V = \frac{1}{2}m^2\phi^2$ on the growth of structure of the universe, in a situation where only a substantial fraction of ultra-light scalar field dark matter constitutes the total dark matter including CDM.

It is well known that the axion as a coherently oscillating scalar field behaves as CDM in cosmologically relevant scales [26]. Khlopov et al. [27] investigated the growth of perturbations due to gravitational instability in a universe dominated by a scalar axion field. The quantum description of cosmological axion perturbations was given by Nambu and Sasaki [28], while the full relativistic description based on the linear perturbation theory was presented in Refs. [29–31]. For a typical mass with 10^{-5} eV the behavior of the axion is equivalent to that of CDM on the cosmological scales including the super-horizon scale [31].

In this work, we consider an axion dark matter model with extremely low mass ($m \leq 10^{-22}$ eV) and investigate the effect of ultra-light axion on the baryon matter density and the CMB anisotropy power spectra and the perturbation growth. Our calculations are based on the full relativistic linear cosmological perturbation theory. Note that some of previous studies on BEC dark matter models relies on Newtonian cosmology and the relativistic description was given only in a limited fashion. Due to the common property of coherent oscillations, our description for the low-mass axion is closely related with that from the BEC or ultra-light scalar field dark matter models.

The structure of this paper is as follows. Section II reviews the basic equations used to describe background and perturbation evolutions based on the relativistic linear perturbation theory, dealing with the multi-component fluids together with the minimally coupled scalar field. In Sec. III the basic properties of the axion dark matter are briefly described. A complete set of perturbation equations for the axion, baryon, and radiation fluids is presented, and initial conditions for the perturbation variables in the early radiation era are derived for two asymptotic limits. Our primary results are summarized in Sec. IV, including baryon matter density and CMB power spectra and the growth of baryon density perturbation for various values of extremely light axion mass. We also compare the cosmological effects of light axion with the CDM model mixed with the massive neutrinos as a hot dark matter component. We discuss our results in Sec. V. Throughout this paper, we set $c \equiv 1 \equiv \hbar$.

II. BASIC EQUATIONS

We consider scalar-type perturbations with the metric [32]

$$ds^2 = -(1 + 2\alpha)dt^2 - 2a\beta_{,\alpha}dt dx^\alpha + a^2 \left[(1 + 2\varphi)g_{\alpha\beta}^{(3)} + 2\gamma_{,\alpha|\beta} \right] dx^\alpha dx^\beta, \quad (1)$$

and introduce

$$\chi \equiv a(\beta + a\dot{\gamma}), \quad \kappa \equiv 3H\alpha - 3\dot{\varphi} - \frac{\Delta}{a^2}\chi. \quad (2)$$

Here $a(t)$ is the cosmic scale factor, $\alpha, \beta, \varphi, \gamma$ are metric perturbations, a dot and a comma indicate the time and spatial derivatives, respectively, and a vertical bar represents the covariant derivative based on the comoving three-space metric $g_{\alpha\beta}^{(3)}$. The energy-momentum tensor is

$$\begin{aligned} T_0^0 &= -\mu - \delta\mu, & T_\alpha^0 &= -\frac{1}{k}(\mu + p)v_{,\alpha}, \\ T_\beta^\alpha &= (p + \delta p)\delta_\beta^\alpha, \end{aligned} \quad (3)$$

where we ignore the anisotropic stress; k is the wave number with $\Delta \equiv -k^2$ in Fourier space.

The background evolution is described by

$$\begin{aligned} H^2 &= \frac{8\pi G}{3}\mu - \frac{K}{a^2} + \frac{\Lambda}{3}, \\ \dot{\mu} + 3H(\mu + p) &= 0, \end{aligned} \quad (4)$$

where $H \equiv \dot{a}/a$ is the Hubble parameter, K is the sign of spatial curvature, and Λ is the cosmological constant. In the multiple component case we have

$$\mu = \sum_j \mu_j, \quad p = \sum_j p_j, \quad (5)$$

and

$$\dot{\mu}_i + 3H(\mu_i + p_i) = 0, \quad (6)$$

where we ignore direct interactions among fluids. For a minimally coupled scalar field we have the equation of motion

$$\ddot{\phi} + 3H\dot{\phi} + V_{,\phi} = 0, \quad (7)$$

and the fluid quantities

$$\mu_\phi = \frac{1}{2}\dot{\phi}^2 + V, \quad p_\phi = \frac{1}{2}\dot{\phi}^2 - V. \quad (8)$$

We need the following equations for the perturbations [32, 33]

$$\dot{\kappa} + 2H\kappa - 4\pi G(\delta\mu + 3\delta p) + \left(3\dot{H} - \frac{k^2}{a^2}\right)\alpha = 0, \quad (9)$$

$$\begin{aligned} \delta\dot{\mu}_i + 3H(\delta\mu_i + \delta p_i) - (\mu_i + p_i) \left(\kappa - 3H\alpha - \frac{k}{a}v_i \right) \\ = 0, \end{aligned} \quad (10)$$

$$\frac{1}{a^4} [a^4(\mu_i + p_i)v_i]' = \frac{k}{a} [(\mu_i + p_i)\alpha + \delta p_i], \quad (11)$$

where

$$\begin{aligned} \delta\mu &= \sum_j \delta\mu_j, & \delta p &= \sum_j \delta p_j, \\ (\mu + p)v &= \sum_j (\mu_j + p_j)v_j. \end{aligned} \quad (12)$$

In the presence of a scalar field we have the equation of motion [33]

$$\begin{aligned} \delta\ddot{\phi} + 3H\delta\dot{\phi} + \frac{k^2}{a^2}\delta\phi + V_{,\phi\phi}\delta\phi \\ = 2\ddot{\phi}\alpha + \dot{\phi}\left(\dot{\alpha} + 6H\alpha + \frac{k^2}{a^2}\chi - 3\dot{\phi}\right), \end{aligned} \quad (13)$$

and the fluid quantities

$$\begin{aligned} (\mu_\phi + p_\phi)v_\phi &= \frac{k}{a}\dot{\phi}\delta\phi, \quad \delta\mu_\phi = \dot{\phi}\delta\dot{\phi} - \dot{\phi}^2\alpha + V_{,\phi}\delta\phi, \\ \delta p_\phi &= \dot{\phi}\delta\dot{\phi} - \dot{\phi}^2\alpha - V_{,\phi}\delta\phi, \end{aligned} \quad (14)$$

with vanishing anisotropic stress.

III. AXION

We consider the axion in the presence of baryonic dust and radiation (photons and neutrinos). The axion is considered as a minimally coupled scalar field with a potential $V = \frac{1}{2}m^2\phi^2$, where m is the axion mass. We strictly ignore H/m higher order term in our analysis. At the current epoch it is

$$\frac{H_0}{m} = 2.133 \times 10^{-28} h \left(\frac{m}{10^{-5} \text{ eV}} \right)^{-1}, \quad (15)$$

where $H_0 \equiv 100h \text{ kms}^{-1}\text{Mpc}^{-1}$ is the Hubble expansion rate at present.

In the axion model the equation of motion leads to the background solution as [29]

$$\phi(t) = a^{-3/2}[\phi_{+0} \sin(mt) + \phi_{-0} \cos(mt)], \quad (16)$$

where ϕ_{+0} and ϕ_{-0} are constant coefficients. We use the fluid formulation of axion. We have

$$\mu_a = \frac{m^2}{2a^3}(\phi_{+0}^2 + \phi_{-0}^2), \quad p_a = 0, \quad (17)$$

thus, the axion behaves as a zero-pressure fluid; for the fluid quantities the time-averaging has been applied for highly oscillating scalar field. For baryon, radiation (as a fluid), and axion, we have

$$\mu = \mu_b + \mu_r + \mu_a, \quad p = \frac{1}{3}\mu_r. \quad (18)$$

To perturbed order, with an ansatz [29]

$$\delta\phi(\mathbf{k}, t) = \delta\phi_+(\mathbf{k}, t) \sin(mt) + \delta\phi_-(\mathbf{k}, t) \cos(mt), \quad (19)$$

the fluid quantities in Eq. (14) give [31]

$$\begin{aligned} \delta\mu_a &= a^{-3/2}m[m(\phi_{+0}\delta\phi_+ + \phi_{-0}\delta\phi_-) \\ &\quad + \frac{1}{2}(\phi_{+0}\delta\dot{\phi}_- - \phi_{-0}\delta\dot{\phi}_+)] - \mu_a\alpha, \\ \delta p_a &= \frac{1}{2}a^{-3/2}m(\phi_{+0}\delta\dot{\phi}_- - \phi_{-0}\delta\dot{\phi}_+) - \mu_a\alpha, \\ \frac{a}{k}(\mu_a + p_a)v_a &= \frac{1}{2}a^{-3/2}m(\phi_{+0}\delta\phi_- - \phi_{-0}\delta\phi_+), \end{aligned} \quad (20)$$

where for the fluid quantities we have taken the time average. Up to this point the perturbed quantities are spatially gauge invariant and the temporal gauge condition has not been taken yet [32].

A. Axion-comoving gauge

As the temporal gauge (hypersurface or slicing) condition we take the axion-comoving gauge [31]

$$(\mu_a + p_a)v_a \equiv 0. \quad (21)$$

Equation (20) gives

$$\frac{\delta\phi_+}{\phi_{+0}} = \frac{\delta\phi_-}{\phi_{-0}} \quad (22)$$

and

$$\frac{\delta\mu_a}{\mu_a} = 2a^{3/2}\frac{\delta\phi_+}{\phi_{+0}} - \alpha, \quad \frac{\delta p_a}{\mu_a} = -\alpha. \quad (23)$$

From Eqs. (9) and (10) for the axion, we have

$$\begin{aligned} \dot{\kappa} + 2H\kappa &= 4\pi G(\mu_b\delta_b + 2\mu_r\delta_r + \mu_a\delta_a) \\ &\quad + \left[12\pi G\left(\mu_b + \frac{4}{3}\mu_r\right) + \frac{k^2 - 3K}{a^2} \right] \alpha, \end{aligned} \quad (24)$$

$$\dot{\delta}_a = \kappa, \quad (25)$$

where $\delta_i \equiv \delta\mu_i/\mu_i$. For the baryon and radiation, under the fluid formulation, Eqs. (10) and (11) give

$$\dot{\delta}_b = \kappa - 3H\alpha - \frac{k}{a}v_b, \quad (26)$$

$$\dot{v}_b + Hv_b = \frac{k}{a}\alpha, \quad (27)$$

$$\dot{\delta}_r = \frac{4}{3}\left(\kappa - 3H\alpha - \frac{k}{a}v_r\right), \quad (28)$$

$$\dot{v}_r = \frac{k}{a}\left(\alpha + \frac{1}{4}\delta_r\right). \quad (29)$$

For a zero-pressure fluid (like a CDM) we have $\alpha = -\delta p/\mu = 0$. Now, in the case of axion, α can be determined in terms of δ_a using Eq. (13). From Eq. (14) we have

$$\delta_a = 2a^{3/2}\frac{\delta\phi_+}{\phi_{+0}} - \alpha, \quad \alpha = -\frac{a^{3/2}k^2}{2m^2a^2}\frac{\delta\phi_+}{\phi_{+0}}. \quad (30)$$

From these two relations, we have [31]

$$\alpha = -\frac{k^2}{4m^2a^2}\frac{1}{1 + \frac{k^2}{4m^2a^2}}\delta_a. \quad (31)$$

Equations (24)–(29) and (31) constitutes the complete set for axion, baryon, and radiation. In a realistic situation we have to use the Boltzmann equations for radiation

(photons and neutrinos) or the tight-coupling approximation for photon-baryon fluid [34, 35]. We note that the above equations are valid in the presence of K and Λ in the background.

From Eqs. (24), (25) and (31) we have

$$\begin{aligned} \ddot{\delta}_a + 2H\dot{\delta}_a - 4\pi G(\mu_a\delta_a + \mu_b\delta_b + 2\mu_r\delta_r) \\ + \left[12\pi G \left(\mu_b + \frac{4}{3}\mu_r \right) + \frac{k^2 - 3K}{a^2} \right] \\ \times \frac{k^2}{4m^2a^2} \frac{1}{1 + \frac{k^2}{4m^2a^2}} \delta_a = 0. \end{aligned} \quad (32)$$

The equation is valid at *all* scales. Ignoring K , and for axion only, we obtain the axion Jeans scale,

$$\lambda_J \equiv \frac{2\pi a}{k_J} = \frac{2\pi}{\sqrt{2\pi G\mu_a + \sqrt{4\pi^2 G^2 \mu_a^2 + 16\pi G\mu_a m^2}}}. \quad (33)$$

In the limit of $k^2/(4m^2a^2) \ll 1$, with present $\Omega_a \equiv 8\pi G\mu_a/(3H^2) \simeq 0.27$, the current Jeans scale becomes [13, 27, 28, 31]

$$\lambda_J = \left(\frac{\pi^3}{G\mu_{a0}m^2} \right)^{1/4} = 50h^{-1/2} \left(\frac{m}{10^{-5} \text{ eV}} \right)^{-1/2} \text{ AU}, \quad (34)$$

which is about the solar system size for $m \sim 10^{-5}$ eV. For extremely low mass axion, we have

$$\lambda_J = 2.4h^{-1/2} \left(\frac{m}{10^{-25} \text{ eV}} \right)^{-1/2} \text{ Mpc}, \quad (35)$$

which is a cosmologically significant scale. On scales larger than the axion Jeans scale the axion behaves as the CDM. In the following we are interested in the observable consequences of such a small mass axion as a dark matter candidate.

B. Initial conditions

In order to have initial conditions for perturbation variables in the early radiation dominated era, we consider the baryon, radiation, and axion in a flat background. In the radiation dominated era ($a \propto t^{1/2}$), Eqs. (24)-(29) give

$$\begin{aligned} \ddot{\delta}_a + \frac{1}{t}\dot{\delta}_a &= \frac{3}{4t^2}\delta_r + \left(\frac{3}{2t^2} + \frac{k^2}{a^2} \right) \alpha, \\ \ddot{\delta}_r + \frac{1}{2t}\dot{\delta}_r + \left(-\frac{1}{t^2} + \frac{k^2}{3a^2} \right) \delta_r &= -\frac{2}{3t}\dot{\delta}_a - \frac{2}{t}\dot{\alpha} + \frac{3}{t^2}\alpha, \\ \ddot{\delta}_b + \frac{1}{t}\dot{\delta}_b &= \frac{3}{4t^2}\delta_r - \frac{3}{2t}\dot{\alpha} + \frac{3}{2t^2}\alpha. \end{aligned} \quad (36)$$

We consider asymptotic solutions in the large-scale limit, thus $k/(aH) \ll 1$.

(I) For $k^2/(m^2a^2) \ll 1$, we have $\alpha = 0$; this is the same as CDM. For $\delta_a \propto t^n$ we have $(n-1)(2n-1)n(n+1) = 0$, thus $n = 1, \frac{1}{2}, 0, -1$, and the growing solution is

$$\delta_a = \delta_b = \frac{3}{4}\delta_r \propto t. \quad (37)$$

This is the same as the adiabatic solution in the case of CDM.

(II) For $k^2/(m^2a^2) \gg 1$, we have $\alpha = -\delta$. For $\delta_a \propto t^n$, we have $(n-1)(n-\frac{1}{2})(n^2+n+\frac{3}{2}) = 0$, and the growing mode is

$$\delta_a = \frac{2}{5}\delta_b = \frac{3}{10}\delta_r \propto t. \quad (38)$$

The condition $k/(ma) \gg 1$ together with $k/(aH) \ll 1$ demands $H/m \gg 1$, thus *violating* our basic assumption of the axion as a coherently oscillating scalar field. Although the numerical integration of the set of equations is possible, the equations are not valid in this case. In the small axion mass we are interested in, such a violation is inevitable at some epoch in the early universe (Sec. IV A). To avoid this difficulty, as a simple solution, though *ad hoc*, we can introduce an evolving axion mass model (Sec. IV B).

IV. OBSERVATIONAL EFFECTS

In this section, we present our numerical calculations of background and perturbation evolutions in the axion dark matter model with extremely low mass. As a fiducial model, we use the flat Λ CDM model consistent with the Wilkinson Microwave Anisotropy Probe 7-year observation ($\Omega_{b0}h^2 = 0.02260$, $\Omega_{c0}h^2 = 0.1123$, $\Omega_\Lambda = 0.728$, $n_s = 0.963$, $\tau = 0.087$) including massless neutrinos with $N_\nu = 3.04$ (see Table 14 of Ref. [2]). As the dark matter component we consider the axion with $\Omega_{a0} = \Omega_{c0}$. In order to calculate the matter and CMB power spectra, we solve a system composed of radiation, baryon, and axion in the axion-comoving gauge. The radiation components are handled by the Boltzmann equations while the photon-baryon fluid by the tight coupling approximation. The detailed numerical methods are presented in Ref. [35].

A. Violation of axion-fluid nature in the early era

Due to the time dependence of H , our basic assumption of $H/m \ll 1$ for axion as a coherently oscillating scalar field is *violated* in the early era especially for a low-mass axion. Top panels of Fig. 1 shows evolutions of H/m and $k/(ma)$ for different values of axion mass and comoving scales. Despite such a violation of the basic axion-fluid assumption, here we present the baryon matter density and CMB anisotropy power spectra for axion

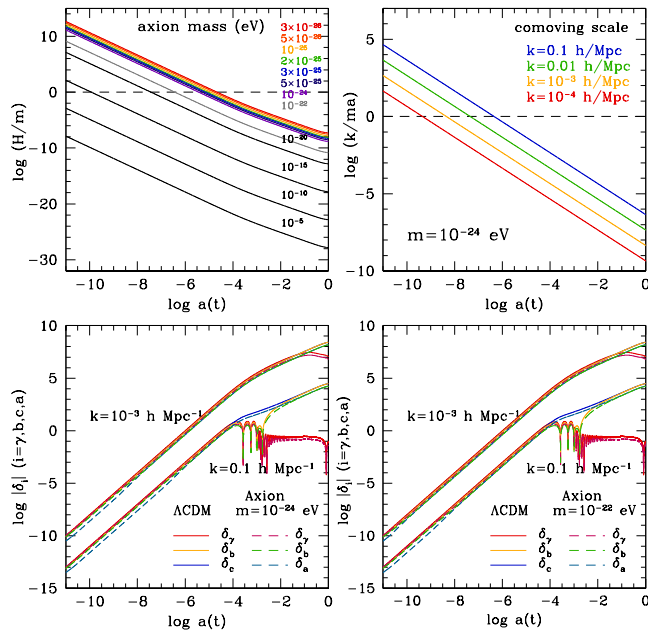


FIG. 1: Top panels: evolution of H/m (left) and $k/(ma)$ (right panel) as a function of scale factor $a(t)$ for different choices of axion mass m and comoving wave number k . The left panel shows that for $m = 10^{-24}$ eV, our basic assumption of $H/m \ll 1$ is violated at $a \lesssim 10^{-5.5}$. On the right panel showing the evolution of $k/(ma)$ for axion mass $m = 10^{-24}$ eV, four different comoving scales from 10^{-4} to $0.1 h\text{Mpc}^{-1}$ have been chosen. Bottom panels: typical evolution of density perturbations δ_i ($i = a, b, c, \gamma$) in the axion-comoving gauge. We considered the ΛCDM model (solid curves) and the Λ -axion-DM model with different choices of axion mass (dashed curves). Here we consider two cases of axion mass, $m = 10^{-24}$ eV (left) and 10^{-22} eV (right panel). In both cases, compared with the cold dark matter in the ΛCDM model (δ_c ; blue solid curve), the axion density perturbation (δ_a ; blue dashed curve) starts to evolve with lower amplitude; see Eq. (38). The behavior of δ_a slightly changes at a certain transition epoch which corresponds to when $k/(ma)$ becomes unity.

with a low mass. In section IV B we will introduce models which avoid such a violation, and will show that the results are similar.

Examples of evolution of individual density perturbation variables are shown in the bottom panels of Fig. 1 (see the caption for detailed descriptions), where the initial conditions for $k/(ma) \gg 1$ limit have been used for the axion mass and the comoving scales considered here. The violation of $H/m \ll 1$ together with the large-scale assumption leads to the transition between $k/(ma) \ll 1$ and $\gg 1$ at the initial epoch (see Fig. 1, top-right panel). In our calculation we have imposed initial conditions for $k/(ma) \gg 1$ presented in Eq. (38) because in most cases of comoving scale and axion mass considered the values of $k/(ma)$ are larger than unity. However, we have checked that the differences in power spectra obtained with different sets of initial conditions in Eqs. (37) and (38) are

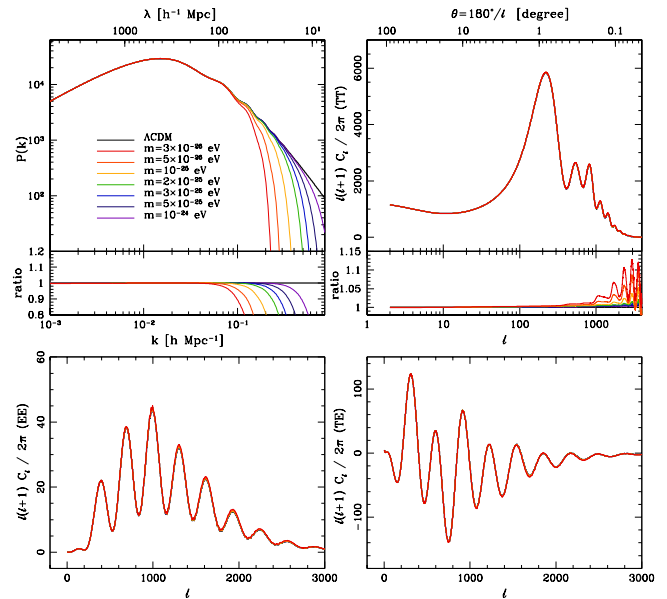


FIG. 2: Baryonic matter (top-left) and CMB temperature, E -mode polarization, TE -cross power spectra (other panels) for axion mass 3×10^{-26} eV $\leq m \leq 10^{-24}$ eV (colored curves). On the top-panels, the ratio of the power spectrum amplitude relative to the fiducial ΛCDM prediction (black curves) are shown to indicate the differences. As the mass decreases below 10^{-24} eV we have strong small-scale suppression of the matter power spectrum due to the increase of axion Jeans scale. The CMB temperature power spectrum show small changes in higher multipoles corresponding to the scales below the axion Jeans scale. Compared with the baryon power spectrum, the change in the CMB power spectrum is minor. No noticeable changes appear in the polarization power spectra.

negligibly small. We also note that if we apply the initial conditions depending on the value of $k/(ma)$ it induces a significant discontinuity in the final power spectra.

The matter and CMB power spectra expected in the low-mass axion model with a mass range 3×10^{-26} eV $\leq m \leq 10^{-24}$ eV are shown in Fig. 2. As expected the small axion mass induces a significant damping in the baryon matter density power spectrum. As the axion mass decreases, the axion Jeans scale increases. From Eq. (35) we can see that for $m \sim 10^{-25}$ eV we have the current Jeans scale $\lambda_J \sim 2.4$ Mpc. However, the damping of the matter power spectrum appears at the comoving scale larger than the current Jeans scale. Note that the critical scale where the damping occurs is determined by the Jeans scale at the radiation-matter equality. Since the comoving Jeans wave number scales with the scale factor as $k_J \propto a^{1/4}$ during the matter era, we expect $k_{J\text{eq}} \approx 0.15 h\text{Mpc}^{-1}$ ($\lambda_{J\text{eq}} \approx 40 h^{-1}\text{Mpc}$) for $\Omega_{a0} = 0.27$ and $a_{\text{eq}} \approx 3 \times 10^{-4}$ (see Fig. 2), see also [11]. Similarly, the CMB power spectra shows the deviation at scales smaller than the axion Jeans scale, thus at very high multipoles; for $m = 3 \times 10^{-26}$ eV, the damping of matter power spectrum occurs around at $k_d \gtrsim 0.1 h\text{Mpc}^{-1}$, which translates into the angu-

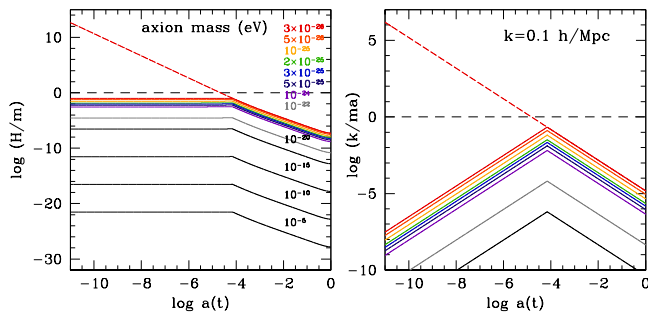


FIG. 3: Evolution of H/m (left) and $k/(ma)$ (right panels) as a function of scale factor $a(t)$ for evolving axion mass model [Eq. (39)]. Here $a_{\text{tr}} = 7 \times 10^{-5}$ has been adopted and the axion mass ranges over $3 \times 10^{-26} \text{ eV} \leq m_0 \leq 10^{-5} \text{ eV}$. On the right panel the variation of $k/(ma)$ is shown for a fixed comoving scale $k = 0.1 \text{ hMpc}^{-1}$ and for axion mass $3 \times 10^{-26} \leq m_0 \leq 10^{-20} \text{ eV}$. For comparison, the case of constant axion mass with $m = 3 \times 10^{-26} \text{ eV}$ is indicated by red dashed curves.

lar scales $\ell = r_{\text{dec}} k_d \gtrsim 1000$ (with $r_{\text{dec}} \approx 10^4 \text{ h}^{-1} \text{Mpc}$ the distance to the decoupling surface); the deviation increases up to 15% at $\ell \sim 3000$ compared to the Λ CDM model (see Refs. [8, 24] for predictions of the CMB anisotropy power spectra based on the BEC and the ultra-light scalar field dark matter models).

B. Evolving axion mass model

We have observed that the condition for axion as a rapidly oscillating scalar field is violated in the early universe. As a simple solution to avoid this problem, we can introduce the evolving axion mass in the early universe. In this way we can investigate the role of constant-low-mass axion in the later evolution of cosmic structures within the axion-fluid formalism. One simple mass-evolution model is to assume that the axion mass varies in proportional to the Hubble parameter before a transition epoch a_{tr} and becomes constant after the transition. In the early epoch of radiation dominated era, the Hubble parameter varies with a^{-2} . Thus, assuming the transition occurs in the radiation era, the evolving axion mass model can be written as

$$m(a) = \begin{cases} m_0(a_{\text{tr}}/a)^2 & a < a_{\text{tr}}, \\ m_0 & a \geq a_{\text{tr}}, \end{cases} \quad (39)$$

where m_0 is the constant axion mass after the transition a_{tr} . Alternatively, we may introduce a evolving axion mass model with smooth variation with e.g., $m(a) = m_0[1 + (a_{\text{tr}}/a)^2]$. Although not shown here, the results are quite similar to those from the simple evolving mass model adopted here. For the results shown in this section, we adopt $a_{\text{tr}} = 7 \times 10^{-5}$, which has been set from the condition that $H/m \approx 0.1$ at $a < a_{\text{tr}}$ for axion mass $m_0 = 3 \times 10^{-26} \text{ eV}$, the lowest axion mass considered in this work. Figure 3 shows evolution of H/m and $k/(ma)$

for different axion mass that varies with this functional form.

C. Effects of small-scale damping on power spectra and growth rate

Here we present the baryonic matter and the CMB anisotropy power spectra, evolution of perturbation variables, and the growth factor based on the simple evolving axion mass model in Eq. (39). The results for the power spectra are shown in Fig. 4 (solid curves), where the power spectra for the constant axion mass (dotted curves; the same as in Fig. 2) are shown for comparison.

Compared to the cases of constant axion mass, the power spectra for varying axion mass shows a small difference: the damping of the power spectrum is slightly less significant as expected. The damping in the matter power spectrum depends on the transition epoch a_{tr} ; more recent transition gives smaller damping. Compared with the Λ CDM fiducial model, the deviation in the CMB anisotropy power spectrum at high multipole ℓ is now to the negative direction. Note that in the case of constant axion mass the deviation appears in the positive direction. In both cases, the magnitude of the maximum deviations are very similar to each other.

In order to determine the low-mass limit of axion we present the baryon density power spectrum in Fig. 5, which shows the substantial small-scale cut-off in the power spectrum for $m < 10^{-22} \text{ eV}$. For $m \geq 10^{-22} \text{ eV}$ the matter power spectrum is almost identical to the CDM case on the scales considered ($\lambda \lesssim 3 \text{ h}^{-1} \text{Mpc}$).

Figure 6 shows the evolutions of density perturbation variables for photon, baryon, and dark matter in the evolving axion mass model at small comoving scales ($k = 0.2$ and 0.5 hMpc^{-1}) and for two extremely small axion mass ($m_0 = 3 \times 10^{-26}$ and $2 \times 10^{-25} \text{ eV}$). In all cases, the initial conditions for $k/(ma) \ll 1$ limit have been used.

In Fig. 7 we show the growth factor $g \equiv \delta_b/a$ (normalized to unity at present) at comoving scales $k = 0.1, 0.5 \text{ hMpc}^{-1}$ and for various axion mass values. At $k = 0.5 \text{ hMpc}^{-1}$, noticeable positive deviations from the Λ CDM prediction are seen. Despite the significant suppression of overall perturbation growth, the recent perturbation growth factor is larger in the low-mass axion model, especially at the small comoving scales. This can be interpreted as the more growth in the axion mass model (see Refs. [9, 10, 21, 25]).

D. Mixed cold and hot dark matter model

The warm dark matter model or the mixture of the cold and hot dark matter model are the alternative candidates to the CDM model with small-scale suppression in the matter power spectra. It would be interesting to

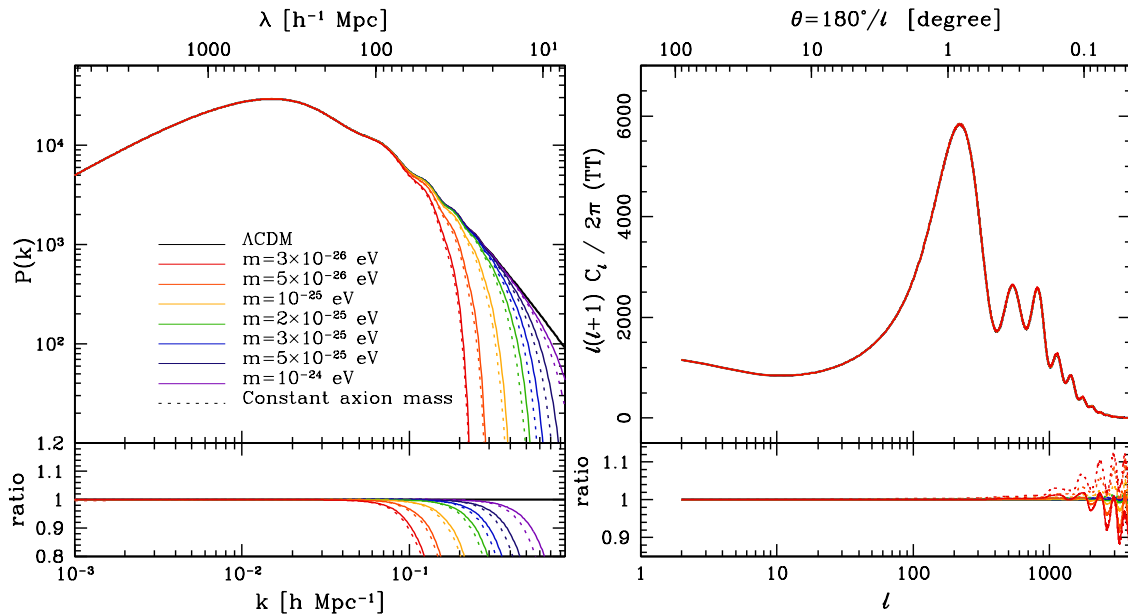


FIG. 4: Baryonic matter (left) and CMB temperature anisotropy (right) power spectra for evolving axion mass model with $a_{\text{tr}} = 7 \times 10^{-5}$ for different axion masses (solid curves). Dotted curves represent the similar power spectra obtained when the constant axion mass is assumed which are the same as those in top panels of Fig. 2. The bottom panels show power ratios relative to the fiducial Λ CDM model prediction. In the CMB power spectrum the deviations at high multipoles ($\ell \gtrsim 1000$) show opposite trends depending on the constant mass and the evolving mass models.

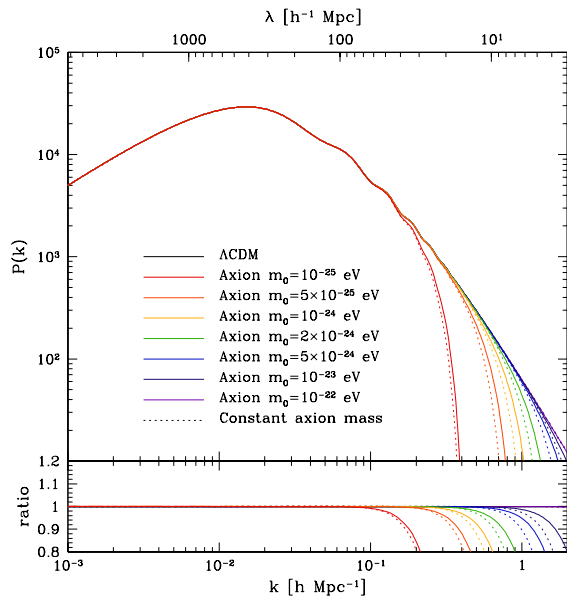


FIG. 5: Baryonic matter density power spectra expected in the evolving axion mass model with $10^{-25} \text{ eV} \leq m_0 \leq 10^{-22} \text{ eV}$ (solid curves). Now the range of comoving wave number has been extended to the higher values (smaller scales) around $k = 2 \text{ hMpc}^{-1}$. Similarly to Fig. 4, the power spectra for the constant axion mass are shown as dotted curves. The bottom panel shows the ratio of power relative to the Λ CDM prediction, indicating the power spectrum damping on small scales.

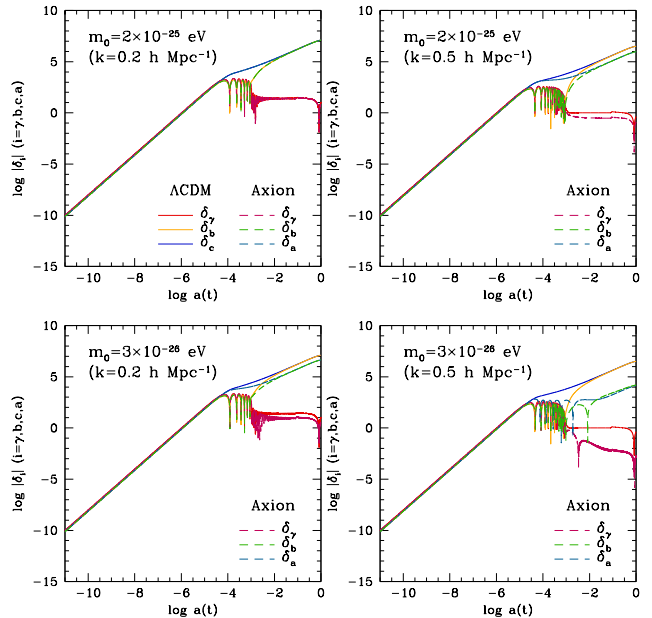


FIG. 6: Evolution of density perturbation variables for photon, baryon, dark matter for evolving axion mass model, Eq. (39) with $a_{\text{tr}} = 7 \times 10^{-5}$. Shown are typical evolutions of density perturbations δ_i ($i = a, b, c, \gamma$) in the axion-comoving gauge for $m_0 = 2 \times 10^{-25}, 3 \times 10^{-26} \text{ eV}$ and $k = 0.2, 0.5 \text{ hMpc}^{-1}$ (dashed curves). We also considered the Λ CDM model whose density perturbations are shown as solid curves in each panel. Compare the results with those in Fig. 1 (bottom panels)

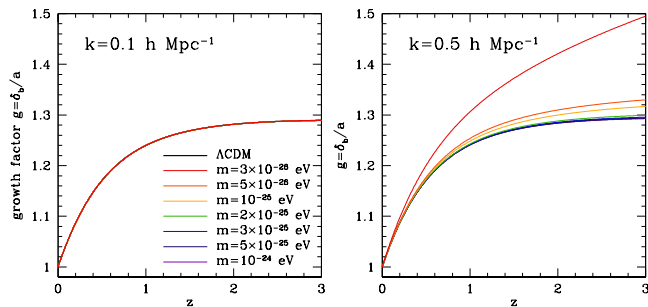


FIG. 7: Evolution of the normalized perturbation growth factor $g \equiv (\delta_b/a)$ at comoving scales of $k = 0.1, 0.5 \text{ hMpc}^{-1}$ for different axion masses (colored curves). Here we use an evolving-axion-mass model with $a_{\text{tr}} = 7 \times 10^{-5}$. Black curves represent the growth factor of the fiducial ΛCDM model.

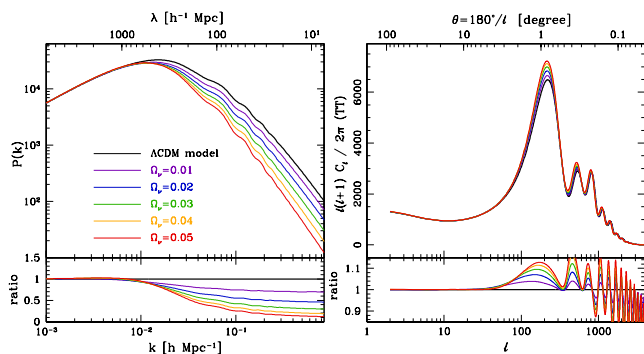


FIG. 8: Matter and CMB temperature anisotropy power spectra expected in a model containing small fraction of massive neutrino component, where we have used the CAMB software [37]. Here we consider massive neutrinos ($N_\nu = 3.04$) whose mass ranges from $m_\nu = 0.154 \text{ eV}$ ($\Omega_{\nu 0} = 0.01$; red) to 0.769 eV ($\Omega_{\nu 0} = 0.05$; violet curves), with a relation $(\Omega_{\nu 0} + \Omega_{c 0})h^2 = 0.1123$. Black curves represent the power spectrum of the fiducial ΛCDM model with massless neutrinos. The curves in the bottom panels indicate the ratios of powers relative to the ΛCDM model prediction.

compare the small-scale suppression of our low-mass axion model with those models. In Fig. 8 we present the case of massive neutrinos contributing as the hot dark matter added to the dominant CDM model. The results are similar to those found in Ref. [36].

Although the low-mass axion dark matter model shows a sharp damping in the baryonic matter power spectrum, the CDM model with a small fraction of massive neutrinos

gives a damping of power with almost constant factor at $k > 0.1 \text{ hMpc}^{-1}$. Besides, the CMB anisotropy power spectrum is very sensitive to the massive neutrino contribution; the massive neutrinos affect all the acoustic oscillatory features at intermediate and high angular scales ($\ell \gtrsim 100$). On the other hand, the behavior of the axion dark matter model is quite different, and is almost insensitive to the axion mass except at the higher multipoles. In the low-mass axion case the changes from the CDM in both power spectra occur only at scales smaller than the axion Jeans scale.

V. DISCUSSION

In this work, we have studied effects of extremely low-mass ($m \leq 10^{-24} \text{ eV}$) axion on the baryon matter density and the CMB anisotropy power spectra, and the perturbation growth based on the full relativistic linear perturbation analysis. With a low mass, however, the basic assumption about the coherently oscillating scalar field is inevitably broken in the early universe ($H/m \gg 1$). We have introduced the simple evolving-axion-mass-in-the-early-universe model to avoid this problem.

We showed that axion mass smaller than 10^{-24} eV induces the characteristic significant damping in the baryon density power spectrum on scales smaller than the axion Jeans scale, and changes in the higher multipole in the CMB anisotropy power spectra. Except for small changes in the higher multipoles ($\ell \gtrsim 1000$) corresponding to the scales smaller than the axion Jeans scale, the CMB power spectrum remains the same as the CDM case. The CDM nature is also preserved in the baryon matter power spectrum above the axion Jeans scale. We showed that the small-scale damping nature of our low-mass axion model differs from the one expected in the CDM model mixed with the massive neutrinos as a hot dark matter component.

Whether the small-scale damping of the baryon matter density power spectrum can help alleviating the excess small-scale clustering problem of the CDM model requires further studies in the nonlinear clustering properties of the light mass axion.

Acknowledgments: J.H. was supported by KRF Grant funded by the Korean Government (KRF-2008-341-C00022). H.N. was supported by grant No. 2010-0000302 from KOSEF funded by the Korean Government (MEST).

[1] R. Amanullah, C. Lidman, D. Rubin, G. Aldering, P. Astier, K. Barbary, M.S. Burns and A. Conley *et al.*, *Astrophys. J.* **716**, 712 (2010); N. Jarosik, C.L. Bennett, J. Dunkley, B. Gold, M.R. Greason, M. Halpern, R.S. Hill and G. Hinshaw *et al.*, *Astrophys. J. Suppl.* **192**, 14 (2011); B.A. Reid, W.J. Percival, D.J. Eisenstein, L. Verde, D.N. Spergel, R.A. Skibba, N.A. Bahcall and T.

Budavari *et al.*, *Mon. Not. Roy. Astron. Soc.* **404**, 60 (2010).
 [2] E. Komatsu, et al. *Astrophys. J. Suppl. Ser.* **192**, 18 (2011).
 [3] J. van Eymeren, C. Trachternach, B.S. Koribalski, and R.-J. Dettmar, *Astron. Astrophys.* **505**, 1 (2009).
 [4] A. Klypin, A.V. Kravtsov, O. Valenzuela, and F. Prada,

- Astrophys. J. **522**, 82 (1999).
- [5] S.-J. Sin, Phys. Rev. D **50**, 3650 (1994); S.U. Ji and S.J. Sin, Phys. Rev. D **50**, 3655 (1994).
- [6] J.-W. Lee and I.-G. Koh, Phys. Rev. D **53**, 2236 (1996); J.-W. Lee, J. Korean Phys. Soc. **54**, 2622 (2009); J.-W. Lee and S. Lim, J. Cosmol. Astropart. Phys. **1001**, 007 (2010).
- [7] F. Ferrer and J.A. Grifols, J. Cosmol. Astropart. Phys. **0412**, 012 (2004); L.A. Ureña-López, J. Cosmol. Astropart. Phys. **0901**, 014 (2009); A.P. Lundgren, M. Bondarescu, R. Bondarescu and J. Balakrishna, Astrophys. J. **715**, L35 (2010); C.G. Böhrer and T. Harko, J. Cosmol. Astropart. Phys. **0706**, 025 (2007); T. Harko, Phys. Rev. D **83**, 123515 (2011); T. Harko, J. Cosmol. Astropart. Phys. **1105**, 022 (2011); P.-H. Chavanis, Phys. Rev. D **84**, 043531 (2011); P.-H. Chavanis and L. Delfini, Phys. Rev. D **84**, 043532 (2011); V. Lora, J. Magaña, A. Bernal, F.J. Sánchez-Salcedo, and E.K. Grebel, J. Cosmol. Astropart. Phys. **1202**, 011 (2012).
- [8] I. Rodríguez-Montoya, J. Magaña, T. Matos, and A. Pérez-Lorenzana, Astrophys. J. **721**, 1509 (2010).
- [9] B. Kain and H.Y. Ling, Phys. Rev. D **85**, 023527 (2012).
- [10] P.H. Chavanis, Astron. Astrophys. **537**, A127 (2012).
- [11] W. Hu, R. Barkana, A. Gruzinov, Phys. Rev. Lett. **85**, 1185 (2000).
- [12] W. Hu, Astrophys. J. **506**, 485 (1998).
- [13] P. Sikivie and Q. Yang, Phys. Rev. Lett. **103**, 111301 (2009).
- [14] O. Erken, P. Sikivie, H. Tam, and Q. Yang, 2012, Phys. Rev. Lett. **108**, 061304 (2012); O. Erken, P. Sikivie, H. Tam, and Q. Yang, Phys. Rev. D **85**, 063520 (2012).
- [15] P.J.E. Peebles and A. Vilenkin, Phys. Rev. D **60**, 103506 (1999); P.J.E. Peebles, Astrophys. J. **534**, L127 (2000).
- [16] T. Matos, F.S. Guzmán and L.A. Ureña-López, Class. Quant. Grav. **17**, 1707 (2000).
- [17] V. Sahni and L. Wang, Phys. Rev. D **62**, 103517 (2000).
- [18] T. Matos and L.A. Ureña-López, Class. Quantum Grav. **17**, L75 (2000); T. Matos and L.A. Ureña-López, Phys. Rev. D **63**, 063506 (2001).
- [19] A. Arbey, J. Lesgourgues, and P. Salati, Phys. Rev. D **64**, 123528 (2001).
- [20] T. Matos, J.-R. Luévano, I. Quiros, L.A. Ureña-López, and J.A. Vázquez, Phys. Rev. D **80**, 123521 (2009).
- [21] A. Suárez and T. Matos, Mon. Not. R. Astron. Soc. **416**, 87 (2011).
- [22] J. Magaña, T. Matos, A. Suárez, F.J. Sánchez-Salcedo, arXiv:1204.5255v1 (2012).
- [23] D.J.E. Marsh and P.G. Ferreira, Phys. Rev. D **82**, 103528 (2010).
- [24] D.J.E. Marsh, E. Macaulay, M. Trebitsch, and P.G. Ferreira, arXiv:1110.0502v1 (2011).
- [25] J. Magaña, T. Matos, V.H. Robles, and A. Suárez, arXiv:1201.6107v1 (2012).
- [26] J. Preskill, M.B. Wise, F. Wilczek, Phys. Lett. B **120**, 127 (1983); L.F. Abbott, P. Sikivie, Phys. Lett. B **120**, 133 (1983); M. Dine, W. Fischler, Phys. Lett. B **120**, 137 (1983); M.S. Turner, Phys. Rev. D **28**, 1243 (1983); J.E. Kim, Phys. Rep. **150**, 1 (1987).
- [27] M.Yu. Khlopov, B.A. Malomed, Ya.B. Zeldovich, Mon. Not. R. Astron. Soc. **215**, 575 (1985).
- [28] Y. Nambu, M. Sasaki, Phys. Rev. D **42**, 3918 (1990).
- [29] B. Ratra, Phys. Rev. D **44**, 352 (1991).
- [30] J. Hwang, Phys. Lett. B **401**, 241 (1997).
- [31] J. Hwang, H. Noh, Phys. Lett. B **680**, 1 (2009).
- [32] J.M. Bardeen, *Particle Physics and Cosmology*, edited by L. Fang, A. Zee (Gordon and Breach, London, 1988) p1.
- [33] J. Hwang, ApJ, **375**, 443 (1991).
- [34] C. Ma and E. Bertschinger, Astrophys. J. **455**, 7 (1995).
- [35] J. Hwang and H. Noh, Phys. Rev. D **65**, 023512 (2001).
- [36] J. Lesgourgues and S. Pastor, Phys. Rep. **429**, 307 (2006).
- [37] A. Lewis and A. Lasenby, Astrophys. J. **513**, 1 (1999); A. Lewis, A. Challinor, and A. Lasenby, Astrophys. J. **538**, 473 (2000).